Nuclear Quantum Effects in H^+ and OH^- Diffusion Along Confined Water Wires

Mariana Rossi,[*,†,¶] Michele Ceriotti,[‡] and David E. Manolopoulos[†]

†*Physical and Theoretical Chemistry Laboratory, University of Oxford, South Parks Road, Oxford OX1 3QZ, United Kingdom*

‡*Laboratory of Computational Science and Modeling, IMX, École Polytechnique Fédérale de Lausanne, 1015 Lausanne, Switzerland*

¶*Current address: Laboratory of Computational Science and Modeling, IMX, École Polytechnique Fédérale de Lausanne, 1015 Lausanne, Switzerland*

E-mail: mariana.rossi@epfl.ch

Abstract

The diffusion of protons and hydroxide ions along water wires provides an efficient mechanism for charge transport that is exploited by biological membrane channels and shows promise for technological applications such as fuel cells. However, what is lacking for a better control and design of these systems is a thorough theoretical understanding of the diffusion process at the atomic scale. Here we focus on two aspects of this process that are often disregarded due to their high computational cost: the use of first principles potential energy surfaces and the treatment of the nuclei as quantum particles. We consider proton and hydroxide ions in finite water wires using density-functional theory, augmented with an apolar cylindrical confining potential. We employ machine learning techniques to identify the charged species, thus obtaining an agnostic definition that takes explicitly into account the delocalization of the charge in the Grotthus-like mechanism. We include nuclear quantum effects (NQE) through the thermostatted ring polymer molecular dynamics method, and model finite system size effects by considering Langevin dynamics on the potential of mean force of the charged species – allowing us to extract the same "universal" diffusion coefficient from simulations with different wire sizes. In the classical case, diffusion coefficients depend significantly on the potential energy surface, in particular on how dispersion forces modulate water-water distances. NQE, however, make the diffusion less sensitive to the underlying potential and geometry of the wire.

Graphical TOC Entry

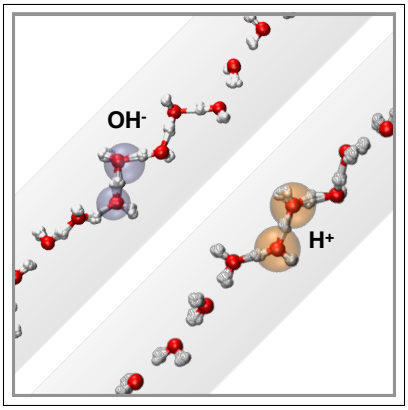

The diffusion and transport of ions, especially protons and hydroxide ions, in aqueous solution or along water wires is a long-standing subject of research. In biological environments, water wires are often the conducting medium for protons or hydroxide ions in channels.[1–6] These channels are involved in a variety of biological processes that deal with the control of pH and charge concentration gradients, mostly for energetic storage. Recently, efforts have also been made to design synthetic pores containing water wires, which are of particular interest for use in fuel cells.[7–11] Even though synthetic pores often bear little resemblance to their biological counterparts (they are, e.g. carbon nanotubes, zeolites, etc.[12]), an understanding of biological pores could bring useful insight into how to modify synthetic pores to make them more efficient at transporting charge. This is just one reason why obtaining a better atomistic understanding of the factors that govern charge transport along water wires is still an active research area.

A great deal of progress has of course already been made. Proton and hydroxide transport in channels is now widely accepted to follow a Grotthus-like mechanism[9,13–15] (or "Zundel–Zundel" mechanism[9]), which is facilitated by the spatial constraint and alignment of the water wire.[3,7–9] However, further study of this mechanism is more challenging than one might expect. First, one needs to use a potential energy surface that allows for bond breaking and making, which is not the case for most empirical potentials. Second, it is known that the self-diffusion coefficient of liquid water at room temperature is increased by around 15% by nuclear quantum effects (NQE).[16] These effects are therefore likely to have at least some impact on proton and hydroxide transport along water wires. And finally, it is necessary to identify the charged species. This is difficult because the identity of the charged species changes during a Grotthus-type rearrangement, and it might well be expected to become even more delocalized and "fuzzy" when nuclear quantum effects are taken into account.[17–20]

The pioneering studies of proton diffusion along water wires were performed using periodic boundary conditions, multistate empirical valence bond (MS-EVB) potentials,[21–23] and classical nuclei. These studies found a proton diffusion constant D of around 4 $\text{Å}^2/\text{ps}$.[7]

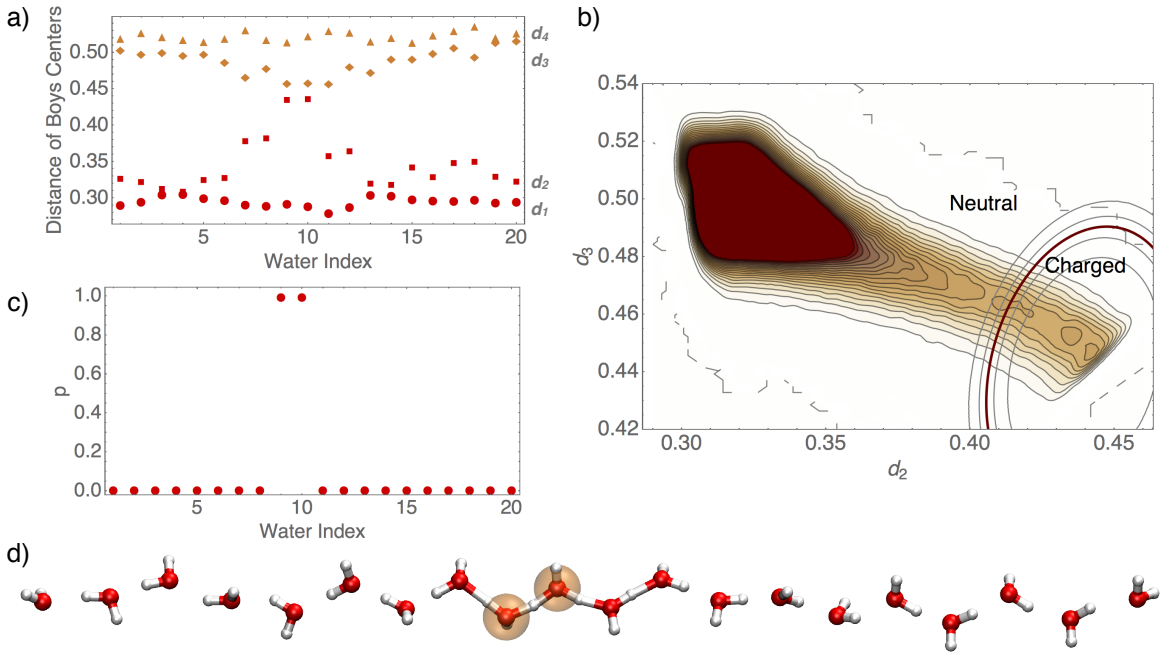

Figure 1: (a) Distribution of Boys center distances from each oxygen in a protonated water wire, for a snapshot of $(H_2O)_{20}H^+$ with BLYP+vdW. Labels for each orbital are shown on the right side of the picture (all but the oxygen core orbitals are shown). (b) Density plot of Boys orbital centers in the d_2 and d_3 coordinates, defined in (a), including all data obtained for the $(H_2O)_{20}H^+$ system (BLYP+vdW, classical nuclei). The isocontours corresponding to 0.1, 0.3, 0.5, 0.7, and 0.9 probability of a point belonging to the charged cluster are also shown, with the 0.5 isocontour highlighted in thick dark red. (c) Posterior probability of each oxygen in the wire belonging to the cluster corresponding to the charged species. (d) Geometry associated with the snapshot discussed in (a) and (c), with orange spheres around the water molecules that are identified as being charged. All distances reported are in Ångstrom.

However, it was subsequently realized that when estimating the diffusion coefficient D of the proton in such a calculation, one should first correct for the slower diffusion of the Bjerrum defect introduced by the periodic boundary conditions, which is coupled to and therefore hinders the proton diffusion.[8] When this was done, the earlier estimates of D were revised upwards to around 17 Å^2/ps.[8] For comparison, the proton diffusion coefficient in bulk liquid water is estimated to be slightly less than 1 Å^2/ps.[14] So protons do indeed diffuse significantly more rapidly along confined water wires than they do in bulk water.

A recent study[24] that combines a classical treatment of the nuclear motion with the BLYP[25,26] density functional finds similar results to those of these earlier MS-EVB studies.

More recently still, a comparison of proton and hydroxide transport along isolated water wires using a potential energy surface fitted to MP2 data has concluded that in shorter wires, hydroxide ions diffuse faster than protons.[27] The diffusion coefficients of both species converge to a similar value of around 32 ± 4 Å^2/ps with increasing system size, but this value is almost twice that given by the MS-EVB and BLYP potentials. Regarding nuclear quantum effects, only static ensemble properties and anecdotal observations related to the diffusion process have so far been reported.[1,11,28,29]

In order to shed further light on the matter, we shall now present a study that investigates the effect of different first principles potential energy surfaces on the diffusion of protons and hydroxide ions along water wires, and that also explicitly accounts for the quantum nature of the nuclear motion. To do this in a computationally tractable fashion, we shall consider relatively short wires containing 20 and 40 water molecules, and we shall avoid the introduction of Bjerrum defects by not imposing periodic boundary conditions. The price to be paid for this is a significant finite size effect that arises from the open-ended boundaries of our wires. We shall eliminate this effect by modeling the diffusion with the Langevin dynamics of a particle moving in the potential of mean force of the charged species in the wire, and show that this allows us to extract diffusion coefficients that are independent of system size and consistent with those obtained in earlier work.

All our calculations were carried out with the i-PI[30] program for the dynamics interfaced with the FHI-aims program[31] for the calculation of first principles energies and forces. We chose to use density-functional theory with the BLYP[25,26] exchange correlation functional and van der Waals (vdW) corrections as proposed in Ref.[32] This choice of functional was based on its overall satisfactory description of several properties of water-based systems when compared to other generalized gradient functionals.[33] We used FHI-aims *light* basis sets and numerical settings for the dynamics (with a 0.5 fs time step for integration), and *tight* settings for the calculation of maximally localized orbitals once every 2 fs. In order to include nuclear quantum effects in our calculations, we used the thermostatted ring polymer

molecular dynamics (TRPMD) method.[34] This provides an efficient way to approximate quantum time correlation functions with first principles forces,[35] and it is especially well suited to calculating zero-frequency properties such as diffusion coefficients.[36] More details on the calculations are given in the supplementary information (SI).

Let us start by tackling the problem of identifying the charged species in our simulations. Maximally localized orbitals are known in electronic structure theory to provide a chemically intuitive picture of lone pairs, bonding pairs and orbital hybridizations. For example in Ref.[37] maximally localized Wannier orbitals have been shown to give different signatures for Eigen and Zundel conformations in charged (protonated) bulk water. We have implemented the calculation of Boys orbitals[38] in the FHI-aims code, following Ref.[39] These orbitals are equivalent to Wannier orbitals[40] in isolated systems. As an example, in Fig. 1 (a) we show the distances of the centers of the Boys orbitals from their nearest oxygen, for one snapshot of a simulation of $(H_2O)_{20}H^+$ with classical nuclei and the BLYP+vdW functional. The geometry of the wire at this snapshot is shown in Fig. 1(d). For most water molecules, one identifies two centers close to each oxygen which are associated with lone pairs (labeled d_1 and d_2) and two centers farther away, which are the bonded orbitals (labeled d_3 and d_4). We do not show the $1s$ orbital as it is always pinned to the center of the oxygen atom. Close to where the proton is located, a delocalized disturbance in the distances d_i can be observed. In order to obtain an unbiased identification of the charged species, we fed these distances into a clustering method based on a Gaussian mixture model for the underlying probability distribution that is optimized to identify different molecular motifs.[41] As in the original work,[41] we call this algorithm "probabilistic analysis of molecular motifs" (PAMM).

In this case, the identification of the charged species based on the underlying probability distribution is challenging, since its probability will have a low intensity compared to that of the neutral waters. We find that the distances d_2 and d_3 are variables where the PAMM algorithm is able to automatically identify two clusters that we assign to the charged and the neutral species. Indeed, the cluster we assign to the charged species appears with a

population of approximately 5 % in the wires of 20 molecules, and with a ratio of approximately 2.5 % for 40 molecules, which is consistent with a 1 in 20 and 1 in 40 picture. In Fig. 1(b), we show a density plot projected on the d_2 and d_3 coordinates from all snapshots of the simulations we have for $(H_2O)_{20}H^+$ with classical nuclei (BLYP+vdW functional). In the same panel, in thick red, we show the isocontour corresponding to a probability of 0.5 of a point belonging to the PAMM cluster we identify as the charged species. This is what effectively separates for us the charged entities from the neutral ones. In Fig. 1(c) we show the posterior probability p_i that each oxygen i belongs to the cluster identified as the charged species, and in Fig. 1(d) we observe that visually this identification makes sense.

Since PAMM defines a probability of a certain entity belonging to one of the clusters it identified, we define the location of the proton or hydroxide ion as $x_{H^+(OH^-)} = \sum_i^{N_O} p_i x_i / \sum_i^{N_O} p_i$, where i runs over the oxygen atoms. In the SI, we compare the position of the proton predicted by PAMM with other commonly adopted definitions in the literature. We note that physically motivated (but empirical) descriptors yield diffusion coefficients essentially equal to PAMM, but more naive choices can yield significantly different results.

We observe that with the PAMM descriptor the proton is mostly localized on a single oxygen (hydronium character) in the classical simulation, and has similar probabilities of being localized on one oxygen or shared between two oxygens (Zundel character) in the quantum simulation, as shown in the SI. This observation is in line with Refs.[18,19] (and other work in the literature), which have found that in the quantum case a "fluxional complex" is a better characterization of the solvated proton. The hydroxide ion has high probabilities of being localized on one oxygen or shared between two in both the classical and quantum simulations, but in the quantum case there is also a non negligible probability it is shared between even more water molecules forming a larger complex (also in line with work reviewed in Refs.[19,20]).

With our descriptor of the charged particle in hand, we can now turn to how to estimate

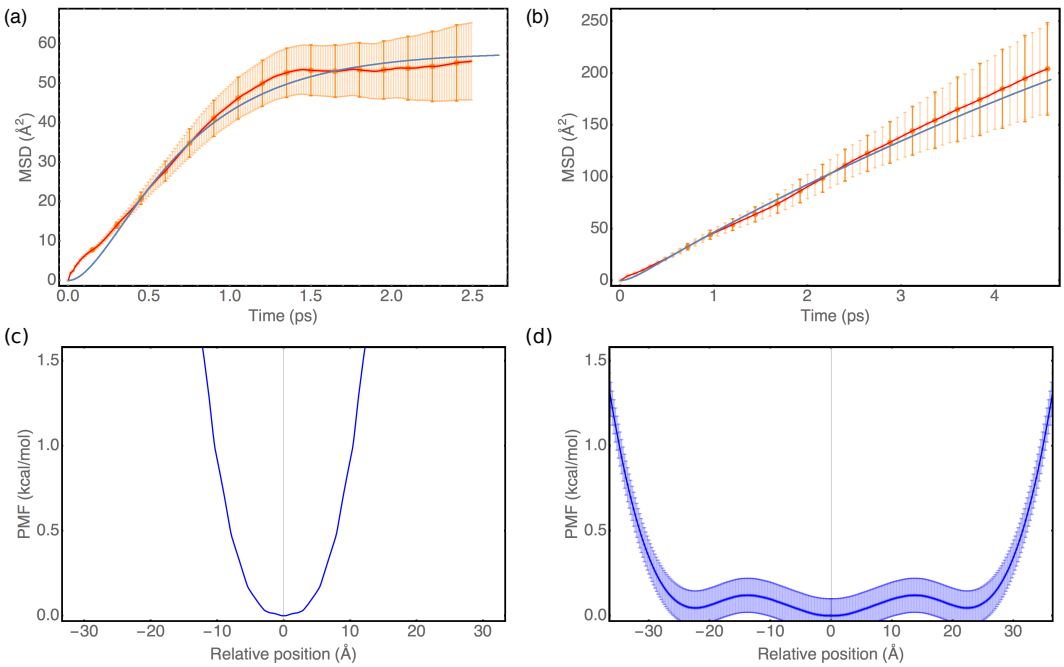

Figure 2: Examples of proton mean square displacements for $(H_2O)_{20}H^+$ in panel (a) and $(H_2O)_{40}H^+$ in panel (b) from *ab initio* (BLYP+vdW, classical nuclei) simulations in red, and corresponding error bars in orange. The blue lines are the best fits obtained for the MSD curves coming from Langevin dynamics in the potential of mean force (see text). Panels (c) and (d): Potentials of mean force corresponding to the simulations shown in the top panels (error bars shown in panel (d), reflecting our limited statistical sampling due to computational cost).

its diffusion coefficient. For an unconstrained particle diffusing in one dimension, the diffusion coefficient D can be calculated from

$$D = \int_0^\infty C_{vv}(t)\, dt = \lim_{t\to\infty} \frac{d\langle \Delta x(t)^2 \rangle}{dt}, \tag{1}$$

where $C_{vv}(t)$ is the velocity autocorrelation function and $\langle \Delta x(t)^2 \rangle$ is the mean square displacement (MSD). In our case, however, the diffusing particle is constrained by the size of the wire. As shown in Fig. 2(a), a typical MSD calculated from the simulations ($(H_2O)_{20}H^+$, BLYP+vdW in this case) looks nothing like the MSD of an unconstrained particle.

There are three regions in the curve in Fig. 2(a). The first region, at times up to 0.3 ps, is not ballistic, deviating from MSD $\propto t^2$ behavior (a very similar behavior for this part

of the curve was observed in all our simulations, with both classical and quantum nuclei). The observed behavior in this region can be attributed to the vibration of the proton in its average environment before the first instance of a Grotthus-like jump. The second region is a transient, close to linear, diffusive region, that extends to around 1.5 ps, and the third region is a saturation region at times larger than 1.5 ps. The saturation is a result of the finite length of the water wire, and its form is determined by the potential of mean force (PMF) experienced by the proton, shown in Fig. 2(c).

This PMF was obtained by building a histogram of the position x of the PAMM particle during the simulations to obtain the corresponding probability density $P(x)$, and calculating $W(x) = -k_B T \ln[P(x)]$. The form of the PMF arises from the interaction of the diffusing particle with the oriented dipoles of the water molecules in the wire, as has been previously discussed in Refs.[8,27] As the length of the wire increases, the PMF in the middle of the wire progressively flattens. However, with first principles potential energy surfaces, we cannot afford both to simulate very long wires and obtain enough statistics to converge the calculation. In fact, this is already clear from the statistics we could gather for $(H_2O)_{40}H^+$ (120 ps of simulations); the PMF in Fig. 2(d) is still slightly wiggly at the bottom. This motivated us to find a model that would allow us to extract diffusion coefficients from finite size wires.

Table 1: Diffusion coefficients calculated for all systems studied in Å^2/ps.

Functional	System	D cl.	D qt.
BLYP+vdW	$(H_2O)_{20}H^+$	39 ± 6	41 ± 5
BLYP+vdW	$(H_2O)_{40}H^+$	30 ± 4	36 ± 6
BLYP	$(H_2O)_{20}H^+$	16 ± 2	41 ± 9
BLYP+vdW	$(H_2O)_{19}OH^-$	33 ± 5	49 ± 8

The simplest way to do this is to note that the potential of mean force provides an effective potential for a Langevin dynamics that approximately accounts for the effect of the environment (in this case the water wire) on the diffusing particle (the charged species).[42] Since for a freely diffusing particle in one dimension the diffusion coefficient is given by

$D = k_B T/(m\gamma)$, where m is the effective mass of the particle and γ is the friction coefficient, the appropriate Langevin equation can be written in terms of D and m as

$$m\ddot{x} = -\frac{dW(x)}{dx} - \frac{k_B T}{D}\dot{x} + \sqrt{2(k_B T)^2/D}\,\xi(t) \tag{2}$$

where $W(x)$ is the PMF of the charged species in the water wire and $\xi(t)$ is a random process such that $\langle \xi(t) \rangle = 0$ and $\langle \xi(0)\xi(t) \rangle = \delta(t)$.

The justification for using this model to fit the simulation data is that (i) it mimics the relevant diffusion process, and (ii) the stationary distribution of the Fokker-Plank equation associated with Eq. (2) is the same as the probability distribution $P(x) = \exp[-W(x)/k_{\mathrm{B}}T]$ obtained from the *ab initio* simulation. However, since it is ballistic at short times, this model is unable to reproduce the more complex dynamics that takes place in the simulations in the initial region of the MSD. A more sophisticated model would be needed to reproduce this region, and also to pin down the effective mass of the diffusing charge. As shown in the SI the model is rather insensitive to changes in the effective mass between 1000 and 2500 a.u., and so it is not possible to determine m by fitting the MSD obtained from Eq. (2) to the results of the simulations. Therefore, in what follows, we have simply set m equal to the mass of a proton ($m = 1836$ a.u.), for both H^+ and OH^-, on the basis that in both cases it is a proton-like entity that diffuses in the Grotthus-like mechanism [1].

In order to estimate the statistical errors in our fitting of the diffusion coefficient, we performed a maximum-likelihood analysis based on the covariance matrix of the *ab initio* MSD data (see the SI for more details). More specifically, we estimated the covariance matrix using the oracle approximating shrinkage algorithm,[43] which is suitable for problems with

[1] We have also considered the over-damped (Brownian) limit of Eq. (2) in which m is set equal to zero,

$$\dot{x} = -\frac{D}{k_B T}\frac{dW(x)}{dx} + \sqrt{2D}\,\xi(t),$$

but found that the resulting MSDs did not fit our simulation data nearly so well as those obtained from Eq. (2) with $m = m_p$ (the mass of a proton).

a smaller number of samples than their dimensionality, and was necessary here to obtain a stable and reliable maximum-likelihood fit.

The goal of this fitting procedure is to find a universal diffusion coefficient that is independent of the boundary conditions present in the simulations. We know, for example, that a naive linear fit of the transient region of the MSD curves would not provide the same D for different lengths of water wire (see the SI). Panels (a) and (b) of Fig. 2 show the best fits of the Langevin model to the simulations for $(H_2O)_{20}H^+$ and $(H_2O)_{40}H^+$ (BLYP+vdW functional); the corresponding diffusion coefficients are reported along with their computed error bars in Table 1. The best fits to all of our other simulations are shown in the SI. Within our error bars, the Langevin model predicts D to be the same for $(H_2O)_{20}H^+$ and $(H_2O)_{40}H^+$, even though the two wires have very different potentials of mean force. We conclude that this procedure is successful in eliminating the finite size effects in the simulations, and we shall now use it to investigate quantum mechanical effects in the water wires.

Our estimated diffusion coefficients from TRPMD simulations of protonated water wires with BLYP+vdW potentials are compared with the classical results in Table 1. We observe that in this case NQEs have hardly any impact on the diffusion coefficient: the quantum and classical Ds are the same to within the computed error bars. We also note that the values we find for $D \approx 36$ Å^2/ps are consistent with those reported in Ref.,[27] which used a potential energy surface fit to the results of MP2 calculations.

Also in Table. 1, we report our estimates for D obtained from classical and quantum simulations of $(H_2O)_{20}H^+$ with the BLYP functional. In this case, we do observe a large nuclear quantum effect. The value of $D \approx 16$ Å^2/ps that we find from the simulation with classical nuclei is consistent with the results of Refs.[8] and,[24] which either used or compared to this functional. However, the value of $D = 41 \pm 9$ Å^2/ps obtained from the TRPMD simulation is roughly twice as large, and in fact it is very similar to the quantum result obtained with the BLYP+vdW functional.

In order to understand the reason for this difference, it is helpful to analyze the free energy

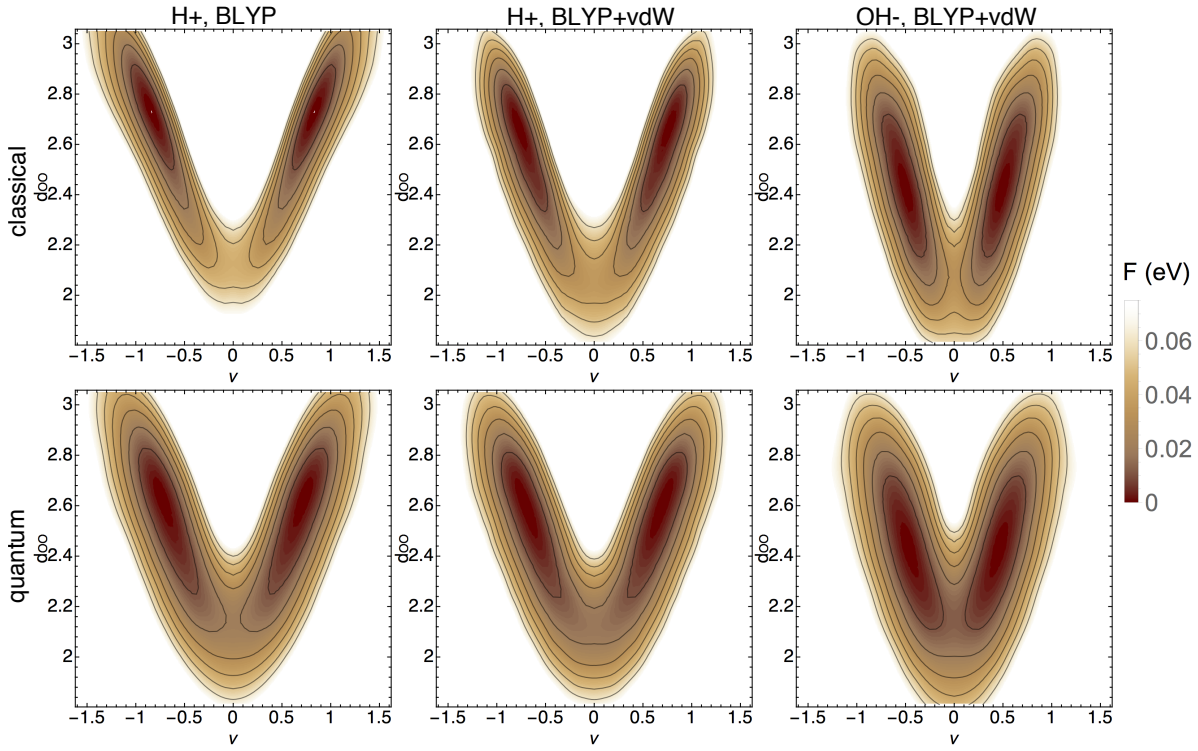

Figure 3: Free energy surfaces for $(H_2O)_{20}H^+$ (with the BLYP and the BLYP+vdW functionals) and $(H_2O)_{19}OH^-$ from classical (top row) and quantum (bottom row) simulations. In the quantum simulations, the bead trajectories were used to construct the probability distribution. Coordinates chosen are the oxygen-oxygen distance d_{OO} and the proton transfer coordinate $\nu = d_{O1-H} - d_{O2-H}$. We calculated $F(\nu, d_{OO}) = -k_B T \ln[P(\nu, d_{OO})]$, where $P(\nu, d_{OO})$ was obtained from a normalized 2D histogram calculated from our simulations, considering all O and H atoms involved in H-bonds in the wire. All distances are in Ångstrom and the contours are drawn for isosurfaces spaced by 10 meV.

surfaces projected on the oxygen-oxygen distance d_{OO} and the proton transfer coordinate $\nu = d_{O1-H} - d_{O2-H}$ for each simulation setup, which we show in Fig.3 considering all O and H atoms involved in H-bonds in the wire. By comparing the classical nuclei simulations of the proton with the BLYP and BLYP+vdW functionals, as well as their decomposition considering only water molecules close to the charge and farther away (shown in Figs. S8 and S9 of the SI), we observe that the barrier for proton transfer is at around 10 meV higher and somewhat broader as a result of the larger O–H^+–O distance in the BLYP case. This suggests that, for the BLYP potential, the rate determining step in the classical diffusion may well be the local proton transfer between two neighbouring oxygens. One would indeed

expect this be accelerated by quantum mechanical tunneling and zero point energy effects, as we have found in our TRPMD simulations. In the BLYP+vdW case, however, the average O–H^+–O distance is shorter, the local proton transfer barrier is lower, this is no longer the rate determining step (which instead involves a collective rearrangement of the water wire), and the quantum mechanical effect on the diffusion coefficient is negligible.

Finally, we also show in Table 1 that in contrast to BLYP+vdW proton diffusion, BLYP+vdW hydroxide diffusion increases slightly on the inclusion of NQEs, to an extent that is statistically significant even with our relatively large error bars. By analyzing Fig. 3, we observe that the free energy surfaces for hydroxide transfer show an overall preference for shorter d_{OO}. The decomposition of the free energies shown in Figs. S9, S10, and S11 of the SI also show a higher barrier for OH^- transfer in the classical case and an overall lower barrier on the ν coordinate in the quantum case, when compared to the proton. As compared to Ref.[18] which treated $H_3O_2^-$, we conclude that both the inclusion of vdW and the extra water molecules can lower barriers substantially in the classical case, but the larger impact of NQE for OH^- is maintained. One caveat we should add here is that GGA functionals tend to underestimate barriers;[33,44] it is possible that the results will change when using hybrid functional. Unfortunately such simulations would be prohibitively demanding in the present context. In any event, our results for the BLYP+vdW density functional do seem to suggest that NQEs enhance OH^- diffusion more than H^+ diffusion along the confined water wires we have considered.

To summarise, we have presented a fully first principles study of the diffusion of proton and hydroxide ions along water wires constrained with an apolar cylindrical potential. We have identified the charged species with the PAMM algorithm, which is unbiased and flexible enough to be used also for more complex systems (such as channels with larger diameters or polar walls). We have also shown how a procedure based on Langevin dynamics on the potential of mean force of the charged species can be used to eliminate finite size effects and obtain a "universal" diffusion coefficient that is the same for both long and short wires.

We find that the details of the electronic structure calculation – in particular the inclusion or neglect of dispersion interactions – have a large impact on the conductivity of water wires in the classical nuclei simulations. This effect is largely determined by how vdW forces modulate the geometry of the wire. One could imagine that similar geometry modulations might be caused by the interaction of the water wire with the channel environment in a more realistic simulation. The inclusion of NQEs in the simulations works as an "equalizing" force, making the diffusion process less sensitive to the potential energy model, and presumably, also to environmental effects (within reasonable fluctuations of the water-water distances). The boundary conditions are another important aspect. Recent measurements[45] of proton transport in small-diameter carbon nanotubes indirectly determine a diffusion coefficient that is more consistent with that obtained by models using periodic boundaries than by models with open-ended wires as we consider here. This stresses the importance, for future studies that wish to connect to experimental data, of a more realistic model of the environment.

Even for the simple model systems we have considered here, it is difficult to gather enough statistics to estimate the diffusion coefficient from *ab initio* simulations using density functional theory, and when this is done the results turn out to be very sensitive to the choice of density functional. It will therefore be essential to find both cheaper and more accurate potentials – for example by training neural networks[46,47] on high level *ab initio* data – in order to obtain quantitative results for more realistic water wires.

Acknowledgement. We would like to thank Christoph Dellago for suggesting Langevin dynamics on the potential of mean force as a means to extract diffusion coefficients from simulations of finite water wires, and to acknowledge computational time awarded from the ARCHER UK National Supercomputing Service Resource Allocation Panel (project e360) and the CSCS Swiss National Computing Center (project s618). MC acknowledges financial support by the Swiss National Science Foundation (project ID 200021-159896) and MR acknowledges funding from the Max Planck Society and from the Deutsche Forschungsgemeinschaft (project RO 4637/1-1).

Supporting Information. Technical details of the simulations, details about our Langevin dynamics model, our fitting procedures and error estimations, and free energy surfaces of the water wires are available.

References

(1) Pomés, R.; Roux, B. Structure and Dynamics of a Proton Wire: A Theoretical Study of H^+ Translocation Along the Single-file Water Chain in the Gramicidin A Channel. *Biophys. J.* **1996**, *71*, 19–39.

(2) Voth, G. A. Computer Simulation of Proton Solvation and Transport in Aqueous and Biomolecular Systems. *Acc. Chem. Res.* **2006**, *39*, 143–150.

(3) Köfinger, J.; Hummer, G.; Dellago, C. Single-file Water in Nanopores. *Biochim. Biophys. Acta* **2011**, *13*, 15403–15417.

(4) Wright, C. Chance and Design - Proton Transfer in Water, Channels, and Bioenergetic Proteins. *Biochim. Biophys. Acta* **2006**, *1757*, 886–912.

(5) Swanson, J.; Maupin, C. M.; Chen, H.; Petersen, M.; Xu, J.; Wu, Y.; Voth, G. Proton Solvation and Transport in Aqueous and Biomolecular Systems: Insights from Computer Simulations. *J. Phys. Chem. B* **2007**, *111*, 4300–4314.

(6) Peng, Y.; Voth, G. A. Expanding the View of Proton Pumping in Cytochrome C Oxidase through Computer Simulation. *Biochim. Biophys. Acta* **2012**, *1817*, 518–525.

(7) Brewer, M.; Schmidt, U.; Voth, G. The Formation and Dynamics of Proton Wires in Channel Environments. *Biophys. J.* **2001**, *80*, 1691–1702.

(8) Dellago, C.; Naor, M.; Hummer, G. Proton Transport through Water-Filled Carbon Nanotubes. *Phys. Rev. Lett* **2003**, *90*, 105902.

(9) Cao, Z.; Peng, Y.; Yan, T.; Li, S.; Li, A.; Voth, G. A. Mechanism of Fast Proton Transport along One-Dimensional Water Chains Confined in Carbon Nanotubes. *J. Am. Chem. Soc.* **2010**, *132*, 11395–11397.

(10) Weinwurm, M.; Dellago, C. Vibrational Spectroscopy of Water in Narrow Nanopores. *J. Phys. Chem. B* **2011**, *115*, 5268–5277.

(11) Chen, J.; Li, X.; Zhang, Q.; Michaelides, A.; Wang, E. Nature of Proton Transport in a Water-filled Carbon Nanotube and in Liquid Water. *Phys. Chem. Chem. Phys.* **2013**, *15*, 6344–6349.

(12) Köfinger, J.; Hummer, G.; Dellago, C. Single-file Water in Nanopores. *Phys. Chem. Chem. Phys.* **2011**, *13*, 15403–15417.

(13) de Grotthuss, C. Memoir on the Decomposition of Water and of the Bodies that it Holds in Solution by Means of Galvanic Electricity. *Biochim. Biophys. Acta* **2006**, *1757*, 871 – 875, Translation and reprint.

(14) Agmon, N. The Grotthuss Mechanism. *Chem. Phys. Lett.* **1995**, *244*, 456 – 462.

(15) Schmitt, U. W.; Voth, G. A. The Computer Simulation of Proton Transport in Water. *J. Chem. Phys.* **1999**, *111*, 9361–9381.

(16) Habershon, S.; Markland, T. E.; Manolopoulos, D. E. Competing Quantum Effects in the Dynamics of a Flexible Water Model. *J. Chem. Phys.* **2009**, *131*, 024501.

(17) Marx, D.; Tuckerman, M. E.; Hutter, J.; Parrinello, M. The Nature of the Hydrated Excess Proton in Water. *Nature* **1998**, *397*, 601–604.

(18) Tuckerman, M. E.; Marx, D.; Klein, M. L.; Parrinello, M. On the Quantum Nature of the Shared Proton in Hydrogen Bonds. *Science* **1997**, *275*, 817–820.

(19) Marx, D.; Chandra, A.; Tuckerman, M. E. Aqueous Basic Solutions: Hydroxide Solvation, Structural Diffusion, and Comparison to the Hydrated Proton. *Chem. Rev.* **2010**, *110*, 2174–2216.

(20) Agmon, N.; Bakker, H. J.; Campen, R. K.; Henchman, R. H.; Pohl, P.; Roke, S.; Thämer, M.; Hassanali, A. Protons and Hydroxide Ions in Aqueous Systems. *Chem. Rev.* **2016**, *116*, 7642–7672.

(21) Schmitt, U. W.; ; Voth, G. A. Multistate Empirical Valence Bond Model for Proton Transport in Water. *J. Phys. Chem. B* **1998**, *102*, 5547–5551.

(22) Day, T. J. F.; Soudackov, A. V.; Čuma, M.; Schmitt, U. W.; Voth, G. A. A Second Generation Multistate Empirical Valence Bond Model for Proton Transport in Aqueous Systems. *J. Chem. Phys.* **2002**, *117*, 5839–5849.

(23) Wu, Y.; Chen, H.; Wang, F.; Paesani, F.; Voth, G. A. An Improved Multistate Empirical Valence Bond Model for Aqueous Proton Solvation and Transport. *J. Phys. Chem. B* **2007**, *112*, 467–482.

(24) Bankura, A.; Chandra, A. Hydroxide Ion Can Move Faster Than an Excess Proton through One-Dimensional Water Chains in Hydrophobic Narrow Pores. *J. Phys. Chem. B* **2012**, *116*, 9744–9757.

(25) Lee, C.; Yang, W.; Parr, R. Development of the Colle-Salvetti Correlation-energy Formula into a Functional of the Electron Density. *Phys. Rev. B* **1988**, *37*, 785–789.

(26) Becke, A. D. Correlation Energy of an Inhomogeneous Electron Gas: A Coordinate-space Model. *J. Chem. Phys.* **1988**, *88*, 1053–1062.

(27) Lee, S. H.; Rasaiah, J. C. Proton Transfer and the Diffusion of H+ and OH- Ions Along Water Wires. *J. Chem. Phys.* **2013**, *139*, 124507.

(28) Hélène Decornez,; Drukker, K.; Hammes-Schiffer, S. Solvation and Hydrogen-Bonding Effects on Proton Wires. *J. Phys. Chem. A* **1999**, *103*, 2891–2898.

(29) Mei, H. S.; Tuckerman, M. E.; Sagnella, D. E.; ; Klein, M. L. Quantum Nuclear ab Initio Molecular Dynamics Study of Water Wires. *J. Phys. Chem. B* **1998**, *102*, 10446–10458.

(30) Ceriotti, M.; More, J.; Manolopoulos, D. E. i-PI: A Python Interface for Ab Initio Path Integral Molecular Dynamics Simulations. *Comp. Phys. Comm.* **2014**, *185*, 1019–1026.

(31) Blum, V.; et al., Ab initio Molecular Aimulations with Numeric Atom-centered Orbitals. *Comp. Phys. Comm.* **2009**, *180*, 2175–2196.

(32) Tkatchenko, A.; Scheffler, M. Accurate Molecular Van Der Waals Interactions from Ground-State Electron Density and Free-Atom Reference Data. *Phys. Rev. Lett.* **2009**, *102*, 073005.

(33) Gillan, M. J.; Alfè, D.; Michaelides, A. Perspective: How Good is DFT for Water? *J. Chem. Phys.* **2016**, *144*, 130901.

(34) Rossi, M.; Ceriotti, M.; Manolopoulos, D. E. How to Remove the Spurious Resonances from Ring Polymer Molecular Dynamics. *J. Chem. Phys.* **2014**, *140*, 234116.

(35) Baldauf, C.; Rossi, M. Going clean: Structure and Dynamics of Peptides in the Gas Phase and Paths to Solvation. *J. Phys. Condens. Matter* **2015**, *27*, 493002.

(36) Habershon, S.; Manolopoulos, D. E.; Markland, T. E.; Miller III, T. F. Ring-Polymer Molecular Dynamics: Quantum Effects in Chemical Dynamics from Classical Trajectories in an Extended Phase Space. *Annu. Rev. Phys. Chem.* **2013**, *64*, 387–413.

(37) Giberti, F.; Hassanali, A. A.; Ceriotti, M.; Parrinello, M. The Role of Quantum Effects on Structural and Electronic Fluctuations in Neat and Charged Water. *J. Phys. Chem. B* **2014**, *118*, 13226–13235.

(38) Boys, S. Construction of Some Molecular Orbitals to Be Approximately Invariant for Changes from One Molecule to Another. *Rev. Mod. Phys.* **1960**, *32*, 296–299.

(39) Guo, Y.; Li, W.; Li, S. An Efficient Linear Scaling Procedure for Constructing Localized Orbitals of Large Molecules Based on the One-particle Density Matrix. *J. Chem. Phys.* **2011**, *135*, 134107.

(40) Marzari, N.; Mostofi, A. A.; Yates, J. R.; Souza, I.; Vanderbilt, D. Maximally Localized Wannier Functions: Theory and Applications. *Rev. Mod. Phys.* **2012**, *84*, 1419–1475.

(41) Gasparotto, P.; Ceriotti, M. Recognizing Molecular Patterns by Machine Learning: An Agnostic Structural Definition of the Hydrogen Bond. *J. Chem. Phys.* **2014**, *141*, 174110.

(42) Allen, M. P.; Tildesley, D. J. *Computer Simulation of Liquids (Oxford Science Publications)*, reprint ed.; Oxford Science Publications; Oxford University Press, 1989.

(43) Chen, Y.; Wiesel, A.; Eldar, Y. C.; Hero, A. O. Shrinkage Algorithms for MMSE Covariance Estimation. *IEEE Trans. Signal Processing* **2010**, *58*, 5016–5029.

(44) Cohen, A. J.; Mori-Sánchez, P.; Yang, W. Challenges for Density Functional Theory. *Chem. Rev.* **2011**, *112*, 289–320.

(45) Tunuguntla, R. H.; Allen, F. I.; Kim, K.; Belliveau, A.; Noy, A. Ultrafast Proton Transport in Sub-1-nm Diameter Carbon Nanotube Porins. *Nature Nano.* **2016**, *11*, 639–644.

(46) Behler, J.; Parrinello, M. Generalized Neural-Network Representation of High-Dimensional Potential-Energy Surfaces. *Phys. Rev. Lett* **2007**, *98*, 146401.

(47) Natajaran, S.; Morawietz, T.; Behler, J. Representing the Potential-energy Surface of Protonated Water Clusters by High-dimensional Neural Network Potentials. *Phys. Chem. Chem. Phys.* **2015**, *17*, 8356-8371.